

Charmed Baryon Spectroscopy from lattice QCD for $N_f = 2 + 1$ flavours

Paula Pérez Rubio*

Institut für Theoretische Physik, Universität Regensburg, D-93040 Regensburg, Germany.

E-mail: paula.perez-rubio@physik.uni-r.de

In recent years, several charmed baryons have been discovered, with more states likely to be found in the future. We investigate the spectra of singly and doubly charmed baryons on the lattice. The spin $J=1/2$ and $J=3/2$ states are calculated for both positive and negative parity.

*Xth Quark Confinement and the Hadron Spectrum,
October 8-12, 2012
TUM Campus Garching, Munich, Germany*

*Speaker.

1. Introduction

Baryons containing heavy quarks provide an interesting laboratory for studying QCD. They combine two different regimes: the slow relative motion of the heavy quarks with the relativistic motion of a light quark. The energies, detectors and luminosities at disposal in experiments made possible the observation of heavy baryons with one heavy quark. The first heavy baryon signal ever seen was the Λ_c^+ at BNL in 1975 followed soon after (1976) by the discovery of Σ_c^{++} at FNAL. Also at Fermilab, in 1981, the first baryon containing a bottom quark Λ_b was observed. Substantial progress has been made, and currently, there is a total of 19 charmed and 5 bottomed baryons in the PDG summary tables [1]. In the last decade, charmed baryons have mainly been observed at the B-factories, whereas new bottom baryons were found at the Tevatron and more recently also at the LHC. Masses, decay form factors, lifetimes and widths have been determined. However, identification of the spin and parity quantum numbers from experiments is still missing; so far, they are assigned based on quark model expectations. It is expected that the large statistics provided by the LHC will allow for their identification through the study of angular distributions of the particle decays. Also, the PANDA experiment at the FAIR facility and the KEK Super-B Factory will look for charmed baryon signals. For doubly heavy baryons, the experimental situation is less favourable. In 2003, Selex [2] published evidence for Ξ_{cc}^+ , but no other experiment has so far confirmed this channel.

Inspired by the experimental activity, many theoretical approaches have been used that try to reproduce the existing spectra and predict new states: for example quark models [3–11], QCD sum rules [12–15], heavy quark effective theory (HQET) based models [16], and lattice QCD (LQCD) [17–24].

In this work, we focus on the study of singly and doubly charmed baryon low lying spectra including positive and negative parity states using 2+1 light dynamical flavours. This is achieved through the Monte Carlo evaluation of a path integral in discretised Euclidean space time with a lattice spacing a . Systematic errors are under control if the ultraviolet cutoff, a^{-1} , is larger than the scales of the problem, the size of the box, L , is larger than the typical size of the hadrons under consideration and an extrapolation to the physical quark masses is performed. Considering the hierarchy of the quark masses and energy scales, for current lattice spacings,

$$m_{\text{light}} < m_s \sim \Lambda < m_c < 1/a < m_b$$

where Λ is the typical hadronic scale. The charm quark mass is below the cutoff and a relativistic calculation of the baryon spectra containing charm quarks is viable. However, it is important to show discretisation errors are under control.

This write-up is organised as follows. In section 2, details of the computational setup are given. In section 3 we briefly describe the methodology used to extract the energy levels. Following this, a detailed list of interpolating operators is given and results are presented in section 4. We finish with some concluding remarks in section 5.

2. Computational details

In our calculations, two different sets of gauge configurations with u/d and s sea quarks were used, 2-HEX [25] and SLiNC [26, 27]. They were generated by the BMW-c and QCDSF collab-

orations, respectively. They were both generated using a gauge action where $O(a^2)$ effects were reduced. The 2-HEX configurations employ tree-level clover Wilson fermions coupled to links with two steps of HEX smearing [28]. This means that the lattice artifacts are reduced to $O(\alpha_s a)$. SLiNC configurations use non-perturbatively clover Wilson fermions with stout link smearing on the derivative terms [29]: $O(a)$ effects are non-perturbatively removed.

The 2-HEX ensembles were generated for a range of lattice spacings from $a \sim 0.092$ fm down to $a \sim 0.054$ fm and pion masses from $M_\pi \sim 520$ MeV down to $M_\pi \sim 120$ MeV. The spatial dimensions cover the range 1.7 – 5.9 fm and the number of configurations per ensemble used for this study is ~ 200 . See [25] for more details. With this set of ensembles we can perform a controlled chiral and continuum extrapolation.

For the SLiNC configurations, there is only one lattice spacing available, $a \sim 0.0795$ fm. The light quark masses were tuned to the $SU(3)_{\text{flavour}}$ -symmetric point, where the flavour singlet mass average $m_q = (m_u + m_d + m_s)/3$ takes its physical value. Then, $m_{u,d}$ and m_s are varied keeping m_q constant [26, 27]. This is motivated by the Gell-Mann - Oakes - Renner relation as well as by $SU(3)$ chiral perturbation theory (χ -PT): m_K approaches its physical value from below, so that it is within the range of applicability of χ -PT ($m_K < 600$ MeV). Ensembles are available for two spatial extents, 1.9 fm and 2.5 fm. So far, we have analysed one of the smaller configurations, with $M_\pi = 348$ MeV and $M_K = 483$ MeV.

3. Methodology

Let $\hat{\mathcal{O}}_1, \hat{\mathcal{O}}_2$ be two interpolating operators that overlap with the baryonic state we are interested in. The correlation function of $\hat{\mathcal{O}}_1$ and $\hat{\mathcal{O}}_2$ is given by,

$$\begin{aligned} C_{\mathbf{p}=0}(\hat{\mathcal{O}}_1, \hat{\mathcal{O}}_2, t) &= \langle \hat{\mathcal{O}}_1(0) \overline{\hat{\mathcal{O}}_2}(t) \rangle = \lim_{T \rightarrow \infty} \frac{1}{Z(T)} \text{Tr} \left[e^{-(T-t)\hat{H}} \hat{\mathcal{O}}_1 e^{-t\hat{H}} \overline{\hat{\mathcal{O}}_2} \right] \\ &= \sum_n \langle 0 | \hat{\mathcal{O}}_1 | n \rangle \langle n | \overline{\hat{\mathcal{O}}_2} | 0 \rangle e^{-E_n t}, \quad Z(T) = \text{Tr} \left[e^{-T\hat{H}} \right], \end{aligned} \quad (3.1)$$

where T is the temporal extent of the lattice. Every correlation function contains contributions from all states with the same quantum numbers. Since we are interested in the low lying spectra, it is desirable to eliminate the contribution of excited states. This can be done using the variational method [30, 31].

3.1 Variational method

The idea is to choose a basis of operators $\hat{\mathcal{O}}_i$ with different overlaps with the state we are interested in. A suitable possibility is to create operators with the same Fock structure and different spatial extent. This can be achieved by applying different numbers of steps of Wuppertal smearing [32, 33] to the fermionic fields. A cross correlation matrix can then be built, $[C(t)]_{ij} = C(\hat{\mathcal{O}}_i, \hat{\mathcal{O}}_j, t)$. Solving the generalised eigenvalue problem (GEVP),

$$C^{-1/2}(t_0) C(t) C^{-1/2}(t_0) v^\alpha(t, t_0) = \lambda^\alpha(t, t_0) v^\alpha(t, t_0). \quad (3.2)$$

It can be shown that the eigenvalues have the following behaviour,

$$\lambda^\alpha(t, t_0) \propto e^{-E_\alpha(t-t_0)} [1 + O(e^{-\Delta E_\alpha t})], \quad \Delta E_\alpha = E_{\alpha'} - E_\alpha, \quad \text{with } \alpha' > \alpha. \quad (3.3)$$

In this way, the lower levels can be extracted cleanly. Nevertheless, there is some freedom of choice of the structure of the interpolating operators. We now motivate the choices made in this work.

3.2 Interpolating operators

To construct sensible interpolating operators overlapping with the baryon states, it is useful to think in terms of their possible inner structure. The constituent quark model guided by the approximate SU(2) or SU(3) flavour symmetry is quite successful when applied to the light quark sector. This statement may no longer be true when we consider heavy baryons. As far as singly charmed baryons are concerned, predictions of HQET tell us that the light degrees of freedom form a diquark and move around the approximately static heavy colour source. In the limit $m_Q \rightarrow \infty$, the total angular momentum of the light diquark becomes a good quantum number. Its total spin s_d takes two possible values, 0 and 1 corresponding to a flavour antisymmetric or symmetric structure, respectively. It is possible to construct operators following these prescription, cf. Table 1.

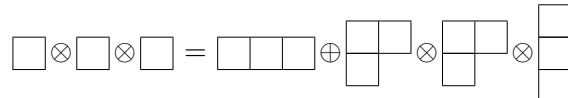
SINGLY CHARMED				$J = \frac{1}{2}$ $J = \frac{3}{2}$		
(S)	(I)	s_d	(qq)Q	\mathcal{O}	Name	Name
(0)	(0)	(0) ⁺	(ll')c	$\mathcal{O}_5 = \varepsilon_{abc}(l^{aT} C \gamma_5 l^b) c^c$	Λ_c	
(0)	(1)	(1) ⁺	(ll)c	$\mathcal{O}_\mu = \varepsilon_{abc}(l^{aT} C \gamma_\mu l^b) c^c$	Σ_c	Σ_c^*
(-1)	($\frac{1}{2}$)	(0) ⁺	(ls)c	$\mathcal{O}_5 = \varepsilon_{abc}(l^{aT} C \gamma_5 s^b) c^c$	Ξ_c	
(-1)	($\frac{1}{2}$)	(1) ⁺	(ls)c	$\mathcal{O}'_\mu = \varepsilon_{abc}(l^{aT} C \gamma_\mu s^b) c^c$	Ξ'_c	Ξ_c^*
(-2)	(0)	(1) ⁺	(ss)c	$\mathcal{O}_\mu = \varepsilon_{abc}(s^{aT} C \gamma_\mu s^b) c^c$	Ω_c	Ω_c^*

Table 1: Summary of quantum numbers of singly charmed baryons and interpolating operators following the HQET approach. l and l' stand for light quarks and S, I and s_d stand for strangeness, isospin, and diquark total spin, respectively. These operators were suggested in [17] for lattice calculations.

As we can see, operators \mathcal{O}_μ (with $s_d = 1$) have contributions from states with total spin $\frac{1}{2}$ and $\frac{3}{2}$. We thus have to use spin projectors to disentangle them. For zero momentum, these projections amount to

$$\begin{aligned}
 (P^{3/2})_{ij} &= \delta^{ij} - \frac{1}{3} \gamma^i \gamma^j, \quad i, j = \{1, 2, 3\}, \\
 (P^{1/2})_{ij} &= \frac{1}{3} \gamma^i \gamma^j.
 \end{aligned} \tag{3.4}$$

Since flavour symmetry is not a good symmetry for charmed baryon systems, in principle it is not clear that interpolating operators falling into the irreducible representations of $SU(4)_{\text{flavour}}$ have a decent overlap with the baryon states. However, these states have also been constructed, and we have seen, cf. section 4, that they lead to results that are compatible with the energy levels obtained from the HQET based interpolating operators. The tensor product of three fundamental representations of $SU(4)_{\text{flavour}}$ is,

$$4 \otimes 4 \otimes 4 = 20_S \oplus 20_M \otimes 20_M \otimes \bar{4}$$


We can construct interpolating operators falling into these multiplets. Since there are at most three different flavours in a baryon, the structure is exactly the same as for the interpolating operators

in the $SU(3)_{\text{flavour}}$ multiplets (with u, d, s quarks). We list the operators corresponding to baryons containing $(ll^{(\prime)}c)$ as constituents.

- $SU(4)$ 20-plet containing $SU(3)$ octets $\begin{array}{|c|c|} \hline \square & \square \\ \hline \end{array}$

$$\Sigma_c: \quad \mathcal{O}_\gamma^P(x) = \varepsilon^{abc} [c^a(x)^T (C\gamma_5) l^b(x)] l_\gamma^c(x).$$

$$\Lambda_c: \quad \mathcal{O}_\gamma^\Lambda(x) = \frac{1}{\sqrt{6}} \varepsilon^{abc} \left\{ 2 [l^a(x)^T (C\gamma_5) l_2^b(x)] c_\gamma^c(x) + [c^a(x)^T (C\gamma_5) l^b(x)] l_\gamma^c(x) - [c^a(x)^T (C\gamma_5) l^b(x)] l_\gamma^c(x) \right\}.$$

$$\Sigma_c^0: \quad \mathcal{O}_\gamma^{\Sigma_c^0}(x) = \frac{1}{\sqrt{2}} \varepsilon^{abc} \left\{ [l^a(x)^T (C\gamma_5) c^b(x)] l_\gamma^c(x) + [l^a(x)^T (C\gamma_5) c^b(x)] l_\gamma^c(x) \right\}.$$

- $SU(4)$ 20-plet containing $SU(3)$ decuplet $\begin{array}{|c|c|c|} \hline \square & \square & \square \\ \hline \end{array}$

$$\Sigma_c^*: \quad \mathcal{O}_\gamma^{\Sigma_c^*}(x) = \varepsilon^{abc} \left\{ 2 (c^{aT} (C\gamma_\mu) l^b) l_\gamma^c + (l^{aT} (C\gamma_\mu) l^b) c_\gamma^c \right\}.$$

$$\Sigma_c^{*0}: \quad \mathcal{O}_\gamma^{\Sigma_c^{*0}}(x) = \frac{\varepsilon^{abc}}{\sqrt{3}} \left\{ (l^{aT} (C\gamma_\mu) l^b) c_\gamma^c + (c^{aT} (C\gamma_\mu) l^b) l_\gamma^c + (l^{aT} (C\gamma_\mu) c^b) l_\gamma^c \right\}.$$

The operators for the baryons with strange content are obtained by substituting the l quark by s in the operators given above.



Figure 1: Structure of a doubly heavy baryon: HQET picture (left), Quarkonium-like picture (right).

Next, we discuss possible interpolating operators for the doubly charmed baryons. In Figure 1, we depict two possible structures for these systems. On the left hand side, the HQET picture, the diquark is formed by the two heavy quarks QQ and interacts with the remaining light quark as if it was a heavy light meson. In this case, the radius of the QQ system is much smaller than Λ^{-1} . The operators reflecting this structure are listed in Table 2.

DOUBLY CHARMED					$J = \frac{1}{2} \quad J = \frac{3}{2}$	
(S)	(I)	s_d	(QQ)q	\mathcal{O}	Name	Name
(0)	(0)	(1)	(cc)l	$\mathcal{O}_\mu = \varepsilon_{abc} (c^{aT} C\gamma_\mu c^b) l^c$	Ξ_{cc}	Ξ_{cc}^*
(-1)	($\frac{1}{2}$)	(1)	(cc)s	$\mathcal{O}_\mu = \varepsilon_{abc} (c^{aT} C\gamma_\mu c^b) s^c$	Ω_{cc}	Ω_{cc}^*

Table 2: Summary of quantum numbers of doubly heavy baryons and interpolating operators following the HQET approach. l, l', S, I and s_d are the same as in Table 1.

On the right hand side, the quarkonium-like picture, the diquark is formed by a heavy and a light quark (Qq) and will interact with the remaining Q as if it was a \bar{Q} . In this case the radius of the QQ system is larger than Λ^{-1} . An example of these operators is given by

$$\Xi_{cc}: \quad \mathcal{O}_\gamma^P(x) = \varepsilon^{abc} [l^a(x)^T (C\gamma_5) c^b(x)] c_\gamma^c(x).$$

Once the correlation functions are constructed out of two interpolating operators, one has to project the correlator into the desired parity, i.e.,

$$C(\hat{\mathcal{O}}_i, \hat{\mathcal{O}}_j, t) = T_{\gamma\gamma} \langle \hat{\mathcal{O}}_{i,\gamma}(0) \overline{\hat{\mathcal{O}}_{j,\bar{\gamma}}(t)} \rangle, \quad (3.5)$$

where T is a polarisation matrix that projects onto positive or negative parity.

4. Results

4.1 Continuum limit

In Figure 2, we present preliminary results for the continuum limit extrapolation of the Ω_c^* and the Ω_{cc} using results from the 2-HEX configurations. A combined fit including the lattice spacing and the light quark mass dependences has been carried out. The following fit function to the baryon masses has been used,

$$y^{\text{FIT}}(a, M_\pi, M_{\bar{s}s} | \mathbf{A}) = y^{\text{cont}} f_X(a) (1 + A_2 x_\pi) (1 + A_3 x_s), \quad (4.1)$$

where $M_{\bar{s}s}$ refers to the strange-strange pseudoscalar and

$$x_\pi = \frac{(M_\pi^{\text{latt}})^2 - (M_\pi^{\text{phys}})^2}{(M_\pi^{\text{phys}})^2}, \quad x_s = \frac{(M_{\bar{s}s}^{\text{latt}})^2 - (M_{\bar{s}s}^{\text{phys}})^2}{(M_{\bar{s}s}^{\text{phys}})^2}. \quad (4.2)$$

For the continuum extrapolation, two fit functions have been used,

$$f_1(a) = 1 + A_1 a^2, \quad f_2(a) = 1 + A_2 a \alpha_s. \quad (4.3)$$

f_1 is also considered since one expects one loop corrections to be small due to the use of smeared links in the action. The errors were estimated using the histogram method combined with the bootstrap statistical analysis [25, 34, 35]. Different fit ranges were chosen and only those with $\chi^2/\text{dof} < 2$ were included.

In Figure 2 the results for the masses of Ω_c^* (left) and Ω_{cc} (right) are shown. To illustrate the quality of the fit, the data points are shifted to the physical light quark mass values and then averaged for each lattice spacing.

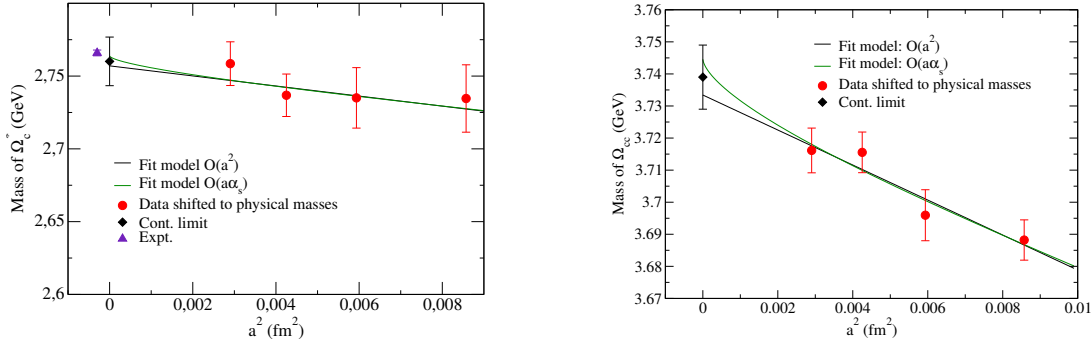


Figure 2: PRELIMINARY. Continuum limit extrapolation from the 2-HEX configurations for Ω_c^* (left) and Ω_{cc} (right) states. The Triangle (violet) stands for the experimental value. The diamonds (black) correspond to the continuum extrapolation and the circles (red) are the simulation data at finite lattice spacing shifted to the physical masses of the light quarks. Two fitting functions have been used, $O(a^2)$ and $O(\alpha_s a)$.

4.2 Spectra

The charmed baryon spectra for the SLiNC ensemble are shown in Figure 3 (left). A 3×3 correlation matrix has been constructed per interpolating operator, with three levels of smearing. We show results for the low lying singly (above) and doubly (below) charmed baryon spectra, including negative parity states, compared with the experimental results. Simulations are still at an early stage and only one combination of light quark masses has been analysed. We can see that the mass differences between baryons containing u, d quarks and the ones with s quarks are

smaller than the experimental values. This is not surprising since we are far from the physical quark masses: the singlet quark mass m_q is tuned to the physical value which means that the u, d and s quark masses are heavier and lighter than their physical values respectively, in spite of the fact that not all systematics are accounted for at present. On the right hand side, we can see a summary of lattice results for the singly (above) and doubly (below) charmed spectra, with different systematics in each case [18–24]. Also, the continuum extrapolated points from the 2-HEX configurations are included. We can see that, overall, lattice results agree with experiment.

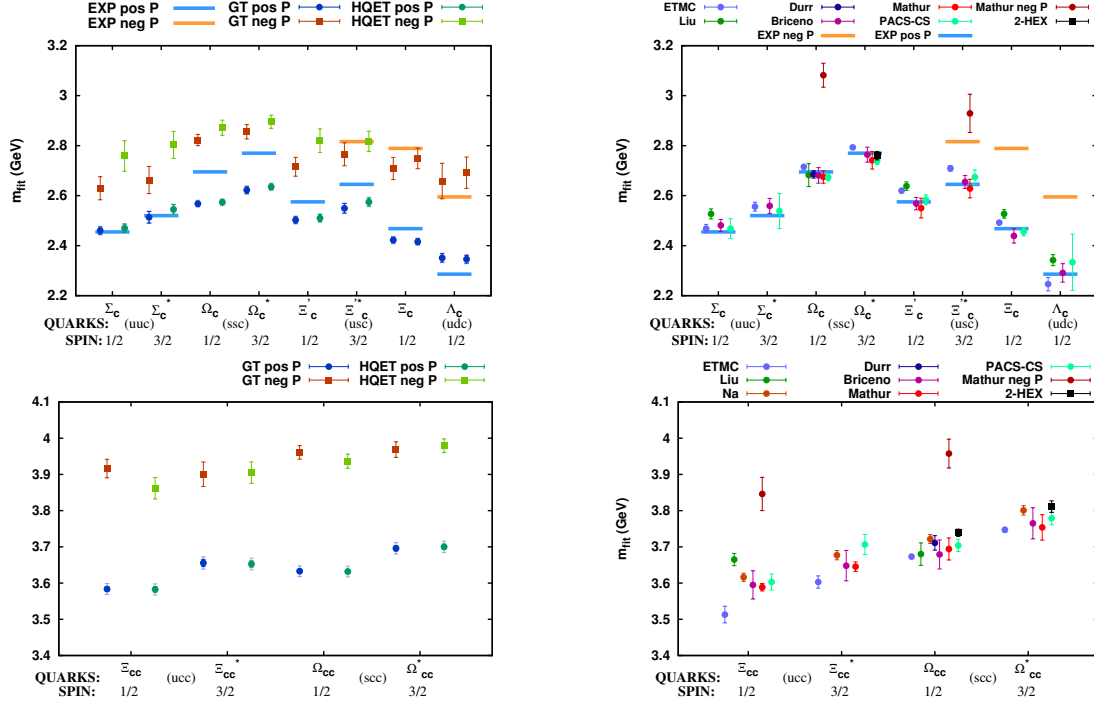


Figure 3: Singly charmed (top) and doubly charmed (bottom) low lying spectrum. On the left hand side, results from the SLiNC configurations are shown ($M_\pi = 348\text{MeV}$). The errors are statistical only. On the right hand side, a summary of lattice results is presented, including results from this work (2-HEX, black squares).

5. Conclusions and outlook

Heavy baryons are good systems to probe QCD dynamics. The last decade witnessed a huge experimental progress in the discovery of new singly heavy baryons. In the near future, spin and parity quantum number identification will be possible, thanks to the large statistics and advanced detectors at the LHC. In the longer term, further progress is expected from planned experiments (PANDA at the FAIR facility and KEK Super-B factory).

In this write-up we have presented preliminary results of an on-going project to obtain the low lying spectra of singly and doubly charmed baryons on the lattice, including states with positive and negative parity. Two different configuration ensembles are being used, employing SLiNC and 2-HEX fermions.

In the near future, we expect to analyse more sets of SLiNC configurations at different quark masses and for larger volumes. For the 2-HEX ensembles we will focus on expanding the analysis to other states.

6. Acknowledgements

The numerical calculations were performed on the SGI Altix ICE machines at HLRN (Berlin-Hannover, Germany), and the BlueGene/P (JuGene) and the Nehalem Cluster (JuRoPA) of the Jülich Supercomputer Center and the iDataCool cluster at Regensburg University. The Chroma software package [36] was used for some of the analysis. I thank my colleagues from the QCDSF and BMW-c collaborations. This work was supported by the EU ITN STRONGnet and the DFG SFB/TR 55.

References

- [1] **Particle Data Group** Collaboration, J. Beringer *et al.* *Phys.Rev.* **D86** (2012) 010001.
- [2] **SELEX** Collaboration, M. Mattson *et al.* *Phys.Rev.Lett.* **89** (2002) 112001.
- [3] L. Copley, N. Isgur, and G. Karl, *Phys.Rev.* **D20** (1979) 768.
- [4] S. Capstick and N. Isgur, *Phys.Rev.* **D34** (1986) 2809.
- [5] R. Roncaglia, D. Lichtenberg, and E. Predazzi, *Phys.Rev.* **D52** (1995) 1722.
- [6] B. Silvestre-Braci, *Few Body Syst.* **20** (1996) 1.
- [7] D. Ebert, R. Faustov, V. Galkin, and A. Martynenko, *Phys.Rev.* **D66** (2002) 014008.
- [8] D. Ebert, R. Faustov, and V. Galkin, *Phys.Rev.* **D72** (2005) 034026.
- [9] W. Roberts and M. Pervin, *Int.J.Mod.Phys.* **A23** (2008) 2817.
- [10] H. Garcilazo, J. Vijande, and A. Valcarce, *J.Phys.* **G34** (2007) 961.
- [11] A. Valcarce, H. Garcilazo, and J. Vijande, *Eur.Phys.J.* **A37** (2008) 217.
- [12] E. Bagan, M. Chabab, H. G. Dosch, and S. Narison, *Phys.Lett.* **B278** (1992) 367.
- [13] E. Bagan, M. Chabab, H. G. Dosch, and S. Narison, *Phys.Lett.* **B287** (1992) 176.
- [14] D.W. Wang, M.q. Huang, and C.z. Li *Phys.Rev.*, **D65** (2002) 094036.
- [15] Z.G. Wang, *Eur.Phys.J.* **C54** (2008) 231.
- [16] E. E. Jenkins, *Phys.Lett.* **B315** (1993) 447.
- [17] **UKQCD** Collaboration, K. Bowler *et al.*, *Phys.Rev.* **D54** (1996) 3619.
- [18] H. Na and S. A. Gottlieb, *PoS LAT2007* (2007) 124.
- [19] L. Liu, H.W. Lin, K. Orginos, and A. Walker-Loud, *Phys.Rev.* **D81** (2010) 094505.
- [20] C. Alexandrou, J. Carbonell, D. Christaras, V. Drach, M. Gravina, *et al.*, *Phys.Rev.* **D86** (2012) 114501.
- [21] R. A. Briceno, H.W. Lin, and D. R. Bolton, *Phys.Rev.* **D86** (2012) 094504.
- [22] S. Dürr, G. Koutsou and T. Lippert, *Phys. Rev. D* **86** (2012) 114514
- [23] S. Basak, S. Datta, M. Padmanath, P. Majumdar, and N. Mathur, *PoS LATTICE2012* (2012) 141.
- [24] Y. Namekawa *et al.* [PACS-CS Collaboration], arXiv:1301.4743 [hep-lat].
- [25] S. Dürr, Z. Fodor, C. Hoelbling, S. Katz, S. Krieg, *et al.*, *JHEP* **1108** (2011) 148.
- [26] W. Bietenholz, V. Bornyakov, N. Cundy, M. Göckeler, R. Horsley, *et al.*, *Phys.Lett.* **B690** (2010) 436.
- [27] W. Bietenholz, V. Bornyakov, M. Göckeler, R. Horsley, W. Lockhart, *et al.*, *Phys.Rev.* **D84** (2011) 054509.
- [28] S. Capitani, S. Dürr, and C. Hoelbling *JHEP* **0611** (2006) 028.
- [29] N. Cundy, M. Göckeler, R. Horsley, T. Kaltenbrunner, A. Kennedy, *et al.*, *Phys.Rev.* **D79** (2009) 094507.
- [30] C. Michael, *Nucl.Phys.* **B259** (1985) 58.
- [31] M. Lüscher and U. Wolff, *Nucl.Phys.* **B339** (1990) 222.
- [32] S. Güsken, U. Löw, K. Mutter, R. Sommer, A. Patel, *et al.*, *Phys.Lett.* **B227** (1989) 266.
- [33] S. Güsken, *Nucl.Phys.Proc.Suppl.* **17** (1990) 361.
- [34] S. Dürr, Z. Fodor, J. Frison, C. Hoelbling, R. Hoffmann, S. D. Katz, S. Krieg and T. Kurth *et al.*, *Science* **322** (2008) 1224
- [35] S. Dürr, Z. Fodor, C. Hoelbling, S. D. Katz, S. Krieg, T. Kurth, L. Lellouch and T. Lippert *et al.*, *Phys. Lett. B* **705** (2011) 477
- [36] **SciDAC**, **LHPC**, **UKQCD** Collaboration, R. G. Edwards and B. Joo, *Nucl.Phys.Proc.Suppl.* **140** (2005) 832.